

# Measuring pitch extractors' response to frequency-modulated multi-component signals

Hideki Kawahara,<sup>1, a</sup> Kohei Yatabe,<sup>2</sup> Ken-Ichi Sakakibara,<sup>3</sup> Tatsuya Kitamura,<sup>4</sup> Hideki Banno,<sup>5</sup> and Masanori Morise<sup>6</sup>

<sup>1</sup>*Center for Innovative Research and Liaison, Wakayama University, Wakayama, 640-8510 Wakayama, Japan*

<sup>2</sup>*Department of Electrical Engineering and Computer Science, Tokyo University of Agriculture and Technology, Tokyo, 184-8588 Tokyo, Japan*

<sup>3</sup>*Department of Speech-Language-Hearing Therapy, Health Science University of Hokkaido, Sapporo, 061-0293 Hokkaido, Japan*

<sup>4</sup>*Faculty of Intelligence and Informatics, Konan University, Kobe, 658-8501 Hyogo, Japan*

<sup>5</sup>*Department of Information Engineering, Meijo University, Nagoya, 468-8502 Aichi, Japan*

<sup>6</sup>*Department of Frontier Media Science, Meiji University, Tokyo, 164-8525 Tokyo, Japan*

(Dated: 5 April 2022)

This article focuses on the research tool for investigating the fundamental frequencies of voiced sounds. We introduce an objective and informative measurement method of pitch extractors' response to frequency-modulated tones. The method uses a new test signal for acoustic system analysis. The test signal enables simultaneous measurement of the extractors' responses. They are the modulation frequency response and the total distortion, including intermodulation distortions. We applied this method to various pitch extractors and placed them on several performance maps. We used the proposed method to fine-tune one of the extractors to make it the best fit tool for scientific research of voice fundamental frequencies.

[<https://doi.org/DOI number>]

[XYZ]

Pages: 1–11

## I. INTRODUCTION

Scientific investigations need reliable and accurate measuring equipment. Pitch extractors are such measuring equipment for investigating the fundamental frequency of voiced sounds. However, since the performance comparison report of pitch extractors in 1993 (Titze, 1993), no comprehensive report has followed despite spite of the increasing number of new pitch extractors. We introduce a new performance report of pitch extractors focusing on response to frequency modulations of voiced sounds. The report uses a method to objectively measure pitch extractors' performance regarding the frequency transfer function, total distortions, and signal-to-noise ratio (Kawahara *et al.*, 2021a,b; Kawahara and Yatabe, 2021). We measured representative pitch extractors and reported raw data, scientific visualization movies, and characterized pitch extractors on performance maps (Kawahara *et al.*, 2022). We propose to use these responses to frequency-modulated multicomponent tones as additional information for evaluating pitch extractors.

This information is also helpful to refine existing pitch extractors. The measurement and visualization of the responses indicated that one of the extractors shows desirable behavior as a measuring tool for detailed

analysis of voice  $f_0$ . We applied the proposed analysis method to fine-tune the extractor (National Institute for Japanese Language and Linguistics (NINJAL) extractor (Kawahara, 2017a; Kawahara *et al.*, 2017) specially designed to conduct a detailed analysis of the CSJ Japanese spontaneous speech corpus (Maekawa, 2003)) to have the best response bandwidth and gain stability regarding the modulation frequency transfer function of frequency-modulated multi-component signals.

In the following sections, we briefly introduce a specific research question that led to the development of the method proposed in this manuscript. Then, we outline the objective measurement procedure with theoretical backgrounds. Followed by descriptions illustrating the principle of operations, we present measurement results of representative pitch extractors and characterize them on performance maps. Based on the measurement and mapping, we selected one pitch extractor, NINJAL, to fine-tune for detailed analysis of voice  $f_0$ . Finally, we discuss further issues and applications. We put technical details and information about the tested pitch extractors in appendices and made the tool open-source.

## II. BACKGROUND AND MOTIVATION

The first author reported the voice-pitch responds to the pitch perturbation of the fed-back voice while the subjects is sustaining a vowel sound in a con-

<sup>a</sup>kawahara@wakayama-u.ac.jp

stant pitch (Kawahara, 1994; Kawahara *et al.*, 1996). The experiment used a realtime pitch changer, harmonizer, with MIDI-controlled perturbation pattern made from a pseudo random signal, named a maximum length sequence (MLS) (Schroeder, 1970). These experiments suggested a consistent compensating response to the perturbation with a relatively short latency (around 100 ms). Following decades, this led to the altered auditory feedback research focusing on pitch-shift paradigm and response with longer latencies (Burnett *et al.*, 1997). This pitch-shift paradigm resulted in many findings (Behroozmand *et al.*, 2012; Larson and Robin, 2016; Patel *et al.*, 2016; Peng *et al.*, 2021; Sivasankar *et al.*, 2005) and led to their neuronal basis (Behroozmand *et al.*, 2020; Chang *et al.*, 2013; Tourville *et al.*, 2008). Unfortunately, possibly because of the technical complexity both in hardware setting and analysis procedures, the response with short latency was less explored (Hain *et al.*, 2000; Zarate *et al.*, 2010).

In addition to the issues mentioned above, the procedure introduced in 1994 had fundamental difficulties. The MLS signal is sensitive to nonlinearity of the tested systems (Burrascano *et al.*, 2019; Farina, 2000; Stan *et al.*, 2002). This susceptibility is problematic because biological systems generally consist of non-linear components. The less sensitive test signal, Swept-sine, is predictable and irrelevant for measuring involuntary response, which is the cause of the short-latency response. The spectral shaping used in the experiment cannot separate the source of the transients caused by the target system and the shaping artifact.

A new test signal, cascaded all-pass filters with randomized center frequencies and phase polarities (CAPRICEP) (Kawahara *et al.*, 2021a,b; Kawahara and Yatabe, 2021), and side-lobe-less Gaussian function solved these difficulties. The new test signal made it possible to simultaneously measure the linear time-invariant (LTI) response and other responses, including harmonic and intermodulation distortions and random and time-varying responses (Kawahara and Yatabe, 2021). Convolution of this new test signal and side-lobe-less Gaussian function made separation of the system transient possible because the test signal has no transients. Moreover, we noticed that voice fundamental frequency responds to some frequency modulated tones (Sivasankar *et al.*, 2005). These phenomena removed the necessity to modulate the fed-back speech sounds in realtime (Kawahara *et al.*, 2021a,b). This removal of feedback signal processing enables investigations on constituent subsystems, pitch perception, and voice  $f_0$  control, separately and non-invasively.

Under usual test conditions, where subjects can aurally monitor their voice pitch, a combination of a band-pass filter with the target  $f_0$  as its center frequency and instantaneous-frequency analysis is enough to conduct the experiment (Kawahara *et al.*, 2021a,b). However, under masked auditory feedback conditions, some subjects could not keep the voice fundamental frequency constant. Sometimes, the voice  $f_0$  deviation exceeded one

octave. This huge deviation made the above-mentioned simple setting fails. This failure motivated us to test existing pitch extractors regarding as measuring equipment. We removed the human subject in the voice response measurement setup and let pitch extractors observe the test sounds directly to investigate pitch extractors' performance.

### III. OBJECTIVE MEASUREMENT

Our target is to observe the fundamental frequency response to auditory stimulation using frequency-modulated speech-like sounds, multi-component harmonic sounds. We need the pitch extractor to behave like measuring equipment with objective specifications of its functions. In this manuscript, we introduce a method to measure the frequency modulation transfer function of the pitch extractor. In addition, we measure spurious responses, including harmonic distortions, intermodulation distortions, and random variations due to noise and other factors. A new test signal made from CAPRICEP (Kawahara and Yatabe, 2021) is the key for this measurement.

#### A. CAPRICEP-based simultaneous measurement

The impulse response of an LTI-system is unique irrespective of test signals. CAPRICEP-based simultaneous measurement takes advantage of this uniqueness. High degrees of freedom for designing CAPRICEP signals enabled us to make a mixture of test signals and separate them into orthogonal signals. Repetitive presentation of the mixture to pitch extractors and the following analysis provide a set of impulse responses to different input signals and observations. The produced impulse responses are not identical. The sample mean and the conditional sample variances yield the LTI-response, the non-linear time-invariant distortions, and random and time-varying responses. In section IV A 4 we introduce details of analysis using CAPRICEP. Details of the mixed-signal generation and orthogonalization are in Appendix A.

#### B. Measurement procedure

The measurement procedure and supporting tools are implemented using MATLAB R2022a (The Mathworks, 2022) running on a PC (Macbook Pro 14 inch 2021, Apple M1 Max, 64GB). Tests using deep-learning-based pitch extractors were conducted on different PC (Mac mini 2020, Apple M1, 16GB) using MATLAB R2021a, Updates 5. We used the live script feature of MATLAB for making visualization movies.

### IV. MEASUREMENT OF PITCH EXTRACTORS

This section describes the underlying signal model, measurement scheme, analysis procedure, and performance indices. We focus on voiced speech analysis especially sustained vowels. We model the discrete-time

speech signal  $s[n]$  as a sum of frequency and amplitude modulated harmonic component and residuals.

$$s[n] = r[n] + \sum_{k=1}^K a_k[n] \sin \left( \varphi[k] + 2\pi k \sum_{m=0}^n f_o[m] t_{\Delta} \right), \quad (1)$$

where  $f_o[n]$  represents the instantaneous frequency of the fundamental component. The symbol  $a_k[n]$  represents the instantaneous amplitude of the  $k$ -th harmonic component. The symbol  $\varphi[k]$  is the initial phase of the  $k$ -th harmonic component. The pitch extractors' objective is to estimate the value of  $f_o[n]$  from the observed voiced sound  $s[n]$ .

## A. Measurement scheme

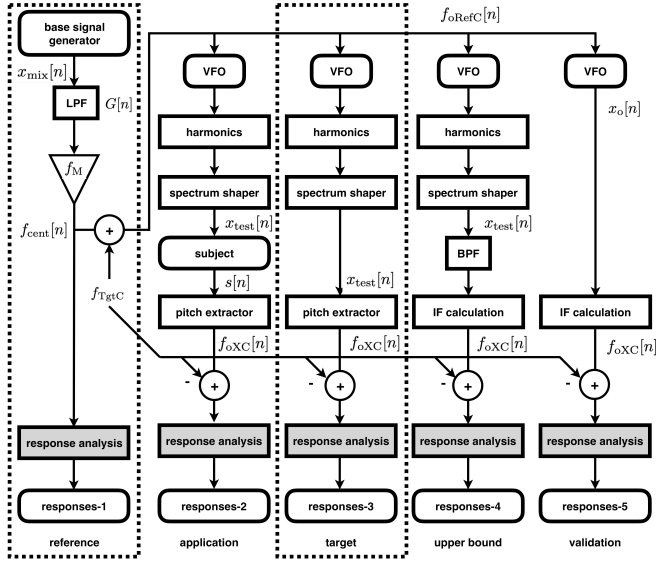


FIG. 1. Measurement scheme and references.

Figure 1 shows the systems we discuss in this article. We use the reference block and the target block to analyze the pitch extractor's responses and performances. The application block represents the voice response experiment described in the background. The validation block is to validate the operation of building blocks. The upper bound block is to check the best possible performance of pitch extractors.

We put symbols of signals discussed in the following section in Fig. 1. The following section defines the signals used in this article.

### 1. Test signal definition

Let  $x_{\text{mix}}[n]$  a base test signal made from three members of CAPRICEP (Appendix A provides details.). We first convolved  $x_{\text{mix}}[n]$  with a side-lobe-less Gaussian

$G[n]$  to generate the frequency modulation signal  $f_{\text{cent}}[n]$ .

$$f_{\text{cent}}[n] = f_M \cdot \frac{x_{\text{mix}}[n] \circ G[n]}{\sigma(x_{\text{mix}}[n] \circ G[n])}, \quad (2)$$

where the symbol  $\circ$  represents convolution and  $f_M$  represents the modulation depth in musical cent. The function  $\sigma(x[n])$  calculates the standard deviation of the signal  $x[n]$ .

The fundamental frequency of the test signal  $f_{\text{oRefC}}[n]$  represented in cent is defined below.

$$f_{\text{oRefC}}[n] = f_{\text{TgtC}} + f_{\text{cent}}[n], \quad (3)$$

where  $f_{\text{TgtC}}$  represents the carrier frequency represented in musical cent. In the following sections, we use  $f_o$  to represent the carrier frequency of the test signal converted from  $f_{\text{oRefC}}[n]$  in musical cent to the linear frequency in Hz.

We use this,  $f_o[n]$ , instantaneous frequency of the fundamental component to generate the fundamental component  $x_o[n]$  and harmonic components  $x_{hk}[n]$ .

$$x_o[n] = \sin \left( 2\pi \sum_{m=0}^n f_o[m] t_{\Delta} \right) \quad (4)$$

$$x_{hk}[n] = \sin \left( 2\pi k \sum_{m=0}^n f_o[m] t_{\Delta} \right), \quad (5)$$

where we removed initial phase in the signal model of speech from the harmonic components of the test signal<sup>1</sup>. The test signal  $x_{\text{test}}[n]$  is a weighted sum of these components.

$$x_{\text{test}}[n] = a_1[n]x_o[n] + \sum_{k=2}^K a_k[n]x_{hk}[n], \quad (6)$$

where we used Japanese vowel spectral shape to define the coefficients  $a_k[n]$ ,  $k = 1, \dots, K$ .

### 2. Test signal generation

Because the target application is a measurement of the fundamental frequency of the sustained voices, we set the length of the test signal to twenty seconds. We set the sampling frequency to 44100 Hz. The response to pitch alternation lasts about one second, and we selected the period of the test signal to  $2^{16} = 65536$  samples, 1.4861 s. It allows us to allocate nine segments of the basic unit of the test signal. The basic unit consists of four possible combinations of three CAPRICEP signals. We overlap and add nine segments on the time axis to generate the base test signal  $x_{\text{mix}}[n]$  separated by 65536 samples. Then, the procedure mentioned-above generated the test signal  $x_{\text{test}}[n]$ . In the following tests, we set the coefficients constant in time  $a_k$ ,  $k = 1, \dots, K$ . We made the target frequency,  $f_{\text{Tgt}}$ , which is represented in Hz and corresponds to  $f_{\text{TgtC}}$  in musical cent, span from 80 Hz to 400 Hz in  $1/48$  octave steps. It resulted in 112 targets.

### 3. Pitch extraction

We fed the test signal to the pitch extractor of interest. We prepared an interface function for each pitch extractor as a MATLAB function. Appendix C shows details. We can test any pitch extractor of interest by writing a similar interface function.

### 4. Response analysis

We converted the extracted fundamental frequency  $f_{oX}[m]$ , where  $m$  represents the analysis frame index, to a discrete-time signal  $f_{oXC}[n]$  of 44100 Hz sampling using linear interpolation represented in the musical cent. Then, we subtracted the target frequency  $f_{TgtC}$  to make the input to response analysis.

The CAPRICEP-based analysis procedure generates six responses  $u_L^{(p)}[n]$  with the length 65536, where  $p$  represents the segment identifier. They are calculated from six periodic segments aligned on the time axis without overlaps. The analysis procedure also generates three set of four responses  $u_S^{(p,j,k)}[n]$  for each segment, where  $j, j = 1, 2, 3$  represents the identifier of the orthogonal sequence and  $k, k = 1, 2, 3, 4$  represents the identifier of the combination. The length of  $h_S^{(p,j,k)}[n]$  is 16384 samples.

We calculated discrete Fourier transform of  $u_L^{(p)}[n]$  and  $u_S^{(p,j,k)}[n]$ . We represent them as  $U_L^{(p)}[k]$  and  $U_S^{(p,j,k)}[k]$ . We also calculate discrete Fourier transform of the reference signal  $u_{RefL}[n]$  and  $u_{RefS}[n]$ . We represent them as  $U_{RefL}[k]$  and  $U_{RefS}[k]$ .

The following equation defines the modulation-frequency transfer function  $H[k]$  of the tested pitch extractor.

$$H[k] = \frac{1}{6} \sum_{p=1}^6 H^{(p)}[k] \quad (7)$$

$$\text{where } H^{(p)}[k] = \frac{U_L^{(p)}[k]}{U_{RefL}[k]}.$$

The following equation defines the sample variance of random and time-varying response  $\sigma_{TV}^2[k]$ .

$$\sigma_{TV}^2[k] = \frac{1}{5} \left| \sum_{p=1}^6 H^{(p)}[k] - H[k] \right|^2, \quad (8)$$

where the denominator  $5 = 6 - 1$  is for the adjustment of the degrees of freedom.

We define the variation of the transfer function for each CAPRICEP signal combination  $\sigma_{nLTI}^{(p,j)}[k]$  using the following equation.

$$\sigma_{nLTI}^{(p,j)}[k] = \frac{1}{2} \sum_{i=1}^3 \left| H^{(p,i,j)}[k] - H^{(p,j)}[k] \right|^2 \quad (9)$$

$$\text{where } H^{(p,j)}[k] = \frac{1}{2} \sum_{i=1}^3 H^{(p,i,j)}[k]$$

$$H^{(p,i,j)}[k] = \frac{U_S^{(p,i,j)}[k]}{U_{RefS}[k]}.$$

Then, we define the sample variance of the non-linear time-invariant response  $\sigma_{nLTI}^2[k]$  using the following equation.

$$\sigma_{nLTI}^2[k] = \frac{1}{6 \times 4} \sum_{p=1}^6 \sum_{j=1}^4 \left( \sigma_{nLTI}^{(p,j)}[k] \right)^2. \quad (10)$$

### B. Performance indices

We introduce four performance indices for characterizing pitch extractors. They are bandwidth  $B_w$ , signal to noise ratio  $SNR_{FM}$ , standard deviations of gain change in frequency  $SD_{fd}$  and in time  $SD_{td}$ . The following sections illustrate these indices with equations and analysis results.

#### 1. Bandwidth

We use the second-order moment to define the bandwidth index  $B_w$ . First, we define the LTI power function  $P_{LTI}[k]$  as the squared absolute value of the transfer function  $P_{LTI}[k] = |H[k]|^2$ , and define the total disturbance power function  $P_{TD}[k]$  as the sum of the non-linear time-invariant response, and random and time-varying response. We select a set of discrete frequency index  $k$  to define the evaluation set  $\Omega = \{k | k \leq k_B\}$  where  $k_B$  is the lowest discrete frequency satisfies  $P_{LTI}[k] < P_{TD}[k]$ . Then, following equation defines  $B_w$ .

$$B_w = \sqrt{\frac{\sum_{k \in \Omega} (f[k])^2 P_{LTI}[k]}{\sum_{k \in \Omega} P_{LTI}[k]}}, \quad (11)$$

where  $f[k]$  represents the function that maps the discrete frequency to the frequency (unit: Hz).

#### 2. Signal to noise ratio

We define the Signal to noise ratio SNR using this bandwidth. The following equation defines  $SNR_{FM}$ .

$$SNR_{FM} = 10 \log_{10} \left( \frac{\sum_{k \in \Omega_{B_w}} P_{LTI}[k]}{\sum_{k \in \Omega_{B_w}} P_{TD}[k]} \right), \quad (12)$$

where  $\Omega_{B_w}$  represents the set of discrete frequencies defined by  $\Omega_{B_w} = \{k | f[k] < B_w\}$ . Note that frequency 0 is not a member of  $\Omega_{B_w}$ .

#### 3. Gain change

The gain representation of the modulation transfer function is a function of the modulation frequency and the signal's fundamental frequency. For measuring equipment, the gain should be constant for pre-defined frequency ranges. We define two performance indices for modulation frequency and fundamental frequency.

The following equation defines the standard deviation of gain change in modulation frequency  $SD_{fd}$ .

$$SD_{fd} = \sqrt{\frac{1}{N_f \Delta f_x} \sum_{k \in \Omega_{10}} \left| 10 \log_{10} \left( \frac{P_{LTI}[k+1]}{P_{LTI}[k]} \right) \right|^2}, \quad (13)$$



where  $\Omega_{10}$  represents the set of discrete modulation frequencies  $\Omega_{10} = \{k|0 < f[k], f[k+1] < 10\}$  (unit: Hz). The symbol  $N_f$  represents the cardinal number of  $\Omega_{10}$  and  $\Delta f_x$  represents the frequency difference of neighboring discrete frequencies. The unit of this index is dB/Hz.

Let  $\overline{P_{LTI}}(f_o[n])$  represents the average gain in  $\Omega_{10}$  for a test signal generated using the  $n$ -th fundamental frequency  $f_o[n]$  Hz. Then, following equation defines the standard deviation of gain change in modulation frequency  $SD_{fd}$ .

$$SD_{td} = \sqrt{\frac{1}{N_t \Delta f_o} \sum_{n \in \Omega_N} \left| 10 \log_{10} \left( \frac{\overline{P_{LTI}}(f_o[n+1])}{\overline{P_{LTI}}(f_o[n])} \right) \right|^2}, \quad (14)$$

where  $\Omega_N$  represents the set of target frequencies  $\Omega_N = \{k|f_L \leq f_o[n], f_o[n] \leq f_H\}$  (unit: semitone). The symbol  $f_L$  represents the lower bound, and  $f_H$  represents the upper bound of the target frequencies. The symbol  $N_t$  represents the cardinal number of  $\Omega_N$  and  $\Delta f_o$  represents the step size of the target frequencies (unit: semitone). The unit of this index is dB/semitone.

## V. RESULTS

We analyzed twenty pitch extractors. Refer to Appendix B for the descriptions of the tested pitch extractors. This section shows representative excerpted responses and summary maps of the statistical analysis results.

### A. Frequency response

Figures 2,3,4,5 show analysis results of several pitch extractors. The thick solid line with legend LTI represents the LTI response  $P_{LTI}[k]$ . The thick dotted line with legend TV-rand represents the sample variance of the random and time-varying response  $\sigma_{TV}^2[k]$ . The dash-dot line with legend non-LTI represents the sample variance of the non-linear time-invariant response  $\sigma_{nLTI}^2[k]$ .

The vertical line annotated by fhL represents the boundary frequency that defines  $\Omega$ . The vertical line annotated by Bw represents the bandwidth  $B_w$ . The horizontal line annotated by TD represents the sum of the non-linear time-invariant response and the random and time-varying response. In the title of the figure, fo represents the target carrier frequency  $f_o$  and FMdpth represents the modulation depth  $f_M$ .

Figure 2 shows the result of a cepstrum-based pitch extractor (Noll, 1967). The total distortion is the highest among four plots. The source of the distortion is the quantization of the estimated fundamental frequency. This method find the peak position on the discrete que-frency bins separated by the signal sampling interval. We found that some of the existing pitch extractors' implementation suffers from this quantization.

There are many ways to circumvent this quantization effect. Figure 3 is such an example. The pitch extractor is one configuration of a popular software tool,

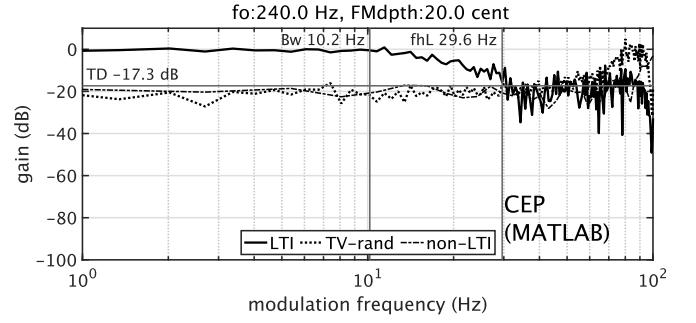


FIG. 2. Response of the cepstrum-based pitch extractor.

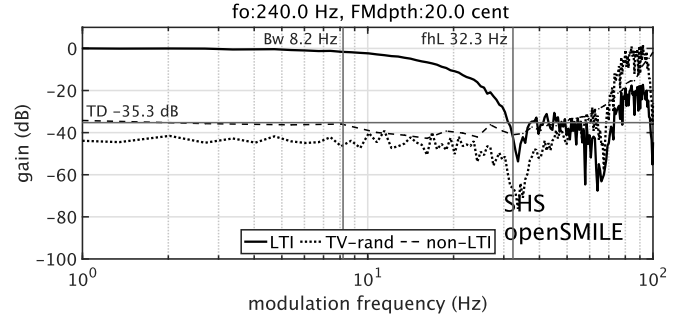


FIG. 3. Response of the subharmonic sampling method in openSMILE.

openSMILE (Eyben *et al.*, 2010a,c), developed for paralinguistic research (Schuller and Batliner, 2013). The pitch extractor uses a classical subharmonic summation-based method (Hermes, 1988) while does not suffer from the quantization effect mentioned above.

Figure 4 shows the result of the default pitch extractor of a popular software tool for doing linguistics using computers, Praat (Boersma and Weenink, 1992–2022). The performance of this pitch extractor is the best of the tested pitch extractors other than ours. The documentation (Boersma and Weenink, 1992–2022) of the tool and personal communication with an author of Praat suggested careful implementation of the underlying algorithm (Boersma, 1993).

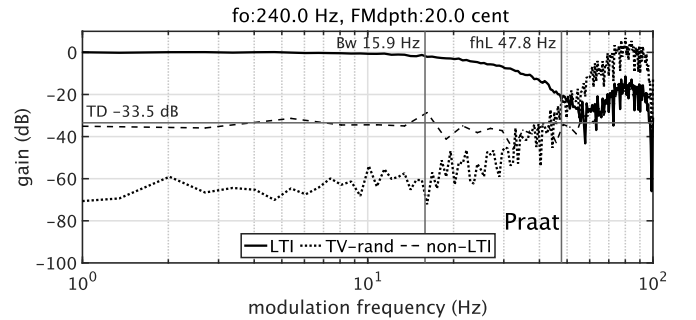


FIG. 4. Response of the Praat's default pitch extractor.

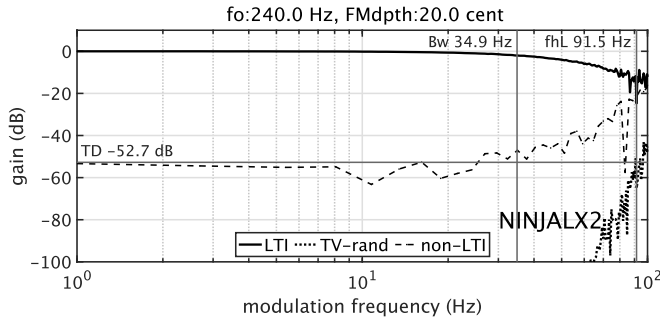


FIG. 5. Response of the NINJAL pitch extractor after fine-tune.

Figure 5 shows the result of an instantaneous-frequency-based pitch extractor NINJAL (Kawahara, 2017a; Kawahara *et al.*, 2017). The total distortion is the lowest, and the bandwidth is the highest. They are close to the upper bound block in Fig. 1. The method has an automatic selection mechanism for the best bandpass filter. The analysis rate also contributes to significantly reducing the random response level. NINJAL calculates the fundamental frequency at the audio sampling rate<sup>2</sup>. Note that we fine-tune the smoothing time constant of the post-processing in NINJAL from 40 ms to 10 ms to get this result.

The measurement of twenty pitch extractors produced 2240 plots. We sequenced each pitch extractor's plots according to the fundamental frequency and converted the aligned plots to a movie to quickly grasp the extractor's behavior. We also gathered sixteen movies and made a movie to inspect them at once. These movies helped us to make the performance indices described above<sup>3</sup>.

## B. Performance map

This section locates tested pitch extractors on maps using derived performance indices. We made two maps. The first map uses the bandwidth and SNR. The second map uses gain variations on the modulation frequency and fundamental frequency axes.

Figure 6 is a scatter plot of the pitch extractors on the modulation frequency bandwidth and SNR plane. Each circle with a character inside represents each pitch extractor. The plot's legend provides a list of extractors with the symbol characters. Note that pitch extractors N to S are ours (One of the authors coded them.). The design target for voice pitch measuring equipment is wider bandwidth and a higher signal-to-noise ratio in the upper right corner of Fig. 6.

Figure 7 is a scatter plot of the pitch extractors regarding gain variation on the modulation frequency dependence plane. The symbols and legend are the same as Fig. 6. For voice pitch measuring equipment, smaller variation in both aspects is desirable. That is the lower-left corner of Fig. 7.

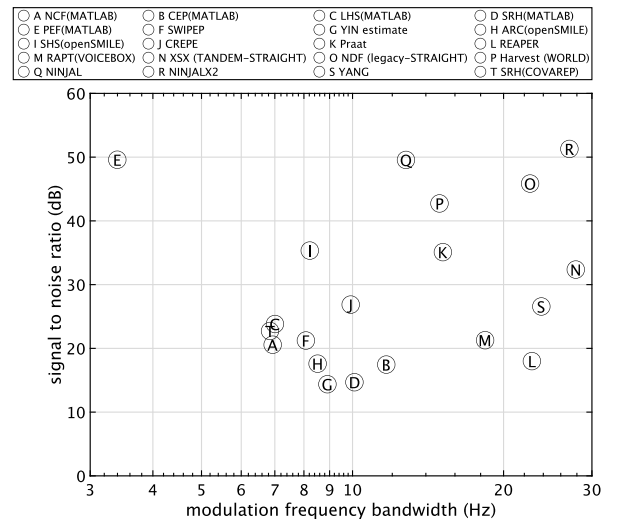


FIG. 6. Pitch extractors location on the bandwidth-SNR map.

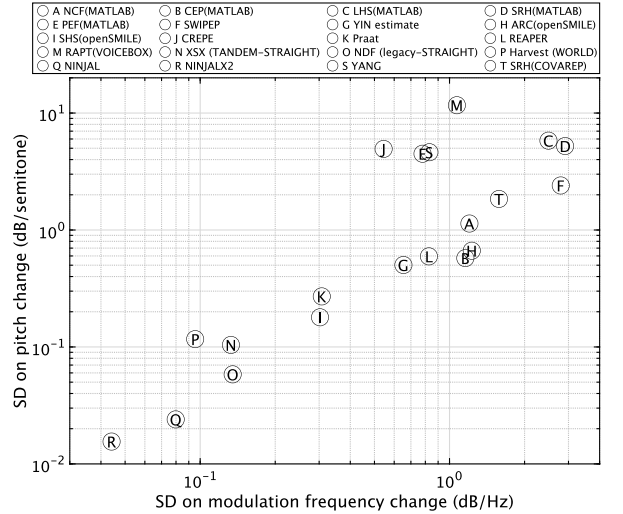


FIG. 7. Pitch extractors location on the gain changes on the modulation frequency-pitch map.

Inspection of Figs. 6 and 7 indicates that pitch extractors N to R form a high-performance cluster. The extractor R is the result of fine-tuning of Q. We changed the smoothing time constant (40 ms in Q) to 10 ms to expand the bandwidth. This change slightly improved SNR and reduced the gain variations. In other words, this change turned the NINJAL pitch extractor into the best fit tool for investigating the fundamental frequency of sustained voiced sounds.

## VI. DISCUSSION

The proposed performance indices are supplemental to existing performance indices. Existing pitch extractors are designed and tuned to their target applica-

tions, for example speech recognition, and speech synthesis under different conditions. The modulation frequency transfer function and other responses used in this manuscript are relevant for investigating sustained voiced sounds recorded in quiet laboratory conditions. Relatively high-performance of our extractors may depend on this difference of target applications.

The underlying signal model causes performance differences. The assumed signal model for this measurement is a variant of the sinusoidal model (McAulay and Quatieri, 1986). We need to explore pitch extractors assuming the other signal models, especially excitation-based models (Kadiri *et al.*, 2021). We also need to explore relations to deep-learning-based pitch extractors. Their underlying models are implicit and tuned through the learning process to improve their target applications' performance. These differences probably contribute to the relatively poor performance of CREPE, which is a deep learning-based pitch extractor.

The proposed tool needs further investigation. We only used spectral shaping with the Japanese vowel /a/. It needs to test other vowels, including foreign ones. The modulation power spectrum of the modulation signal  $f_{\text{cent}}[n]$  is different from that of natural voices (Titze, 1993). We need to test pitch extractors when nonlinearity is not negligible, using test signals having the same acoustic parameters as the voiced sounds in question.

Even with these issues, the proposed measuring tool and the performance indices introduce a new point of view on the old and still hot topic, pitch extraction. We open-sourced the tool and provided an easy means to apply the tool to any pitch extractors of interest. A brief description is in Appendix C.

## VII. CONCLUSION

We introduced an objective measurement method of pitch extractors' response to frequency-modulated multi-component tones. We introduced performance indices based on the method. The proposed performance indices provide new and supplemental means for existing performance measures. We measured representative pitch extractors and selected one of them for further refinement to make it a valuable tool for investing voice  $f_0$  response to auditory stimulation. We open-sourced the proposed tool to make researchers easily select and tune pitch extractors for their research purposes.

## ACKNOWLEDGMENTS

We appreciate Heiga Zen of Google Brain and Kikuo Maekawa of NINJAL for inviting the first author for their projects. Participating in their projects enabled us to develop the reference pitch extractor NINJAL. The naming is an acknowledgment for the Center for Corpus Development, NINJAL. This research was supported by Grants in Aid for Scientific Research (Kakenhi) by JSPS numbers, JP18K00147, JP18K10708, JP19K21618, JP21H03468, JP21H04900, and JP21H00497.

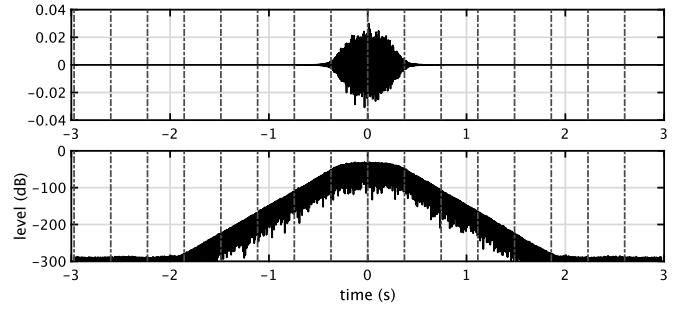


FIG. 8. Waveform and level of an unit-CAPRICEP. Vertical dash-dot lines represents allocation interval.

## APPENDIX A: CAPRICEP-BASED MEASUREMENT

An element of CAPRICEP signals is an all-pass filter. We call it a unit-CAPRICEP. The transfer function of unit-CAPRICEP is a product of second-order IIR filters. Using two random numbers, we allocate each all-pass filter's transfer function and its complex conjugate. The allocation rule is a generalized version of the rule of velvet noise (Välimäki *et al.*, 2013). The generalization enabled the flexible design of the envelope shape of unit-CAPRICEP (Kawahara and Yatabe, 2021). Figure 8 shows an example shape and level of unit-CAPRICEP.

We select three elements  $x_{\text{CP}}^{(1)}[n]$ ,  $x_{\text{CP}}^{(2)}[n]$ , and  $x_{\text{CP}}^{(3)}[n]$  to prepare three sequences. Then, we generate three base sequences  $x_{\text{B}}^{(1)}[n]$ ,  $x_{\text{B}}^{(2)}[n]$ , and  $x_{\text{B}}^{(3)}[n]$  using following equation.

$$x_{\text{B}}^{(k)}[n] = \sum_{m \in \mathbb{Z}} B[m \bmod 4, k] x_{\text{CP}}^{(k)}[n + mN_p] \quad (\text{A1})$$

$$B = \begin{bmatrix} 1 & 1 & 1 \\ 1 & -1 & 1 \\ 1 & 1 & -1 \\ 1 & -1 & -1 \end{bmatrix}, \quad (\text{A2})$$

where  $N_p$  represents the allocation interval in samples. The sum of these three sequences  $x_{\text{B}}^{(k)}[n]$ , ( $k = 1, 2, 3$ ) is the base test signal  $x_{\text{mix}}[n]$  in Eq.(2).

Figure 9 shows signal processing process starting from the mixed signal, the base test signal  $x_{\text{mix}}[n]$  in Eq.(2). Convolution of time reversed version of each element  $x_{\text{CP}*}^{(k)}[n] = x_{\text{CP}}^{(k)}[-n]$  and the base test signal recovers periodically allocated pulses with the polarity defined by  $B$ . The resulted signal also consists of temporally spread noise-like cross-correlation between the other sequences. That is the second plot of Fig. 9.

Periodic shift and add operation using  $B$  as coefficient completely cancel these correlations and recover three orthogonal sequences. This procedure produces four segments consisting of a unit pulse for each sequence. In other words, the procedure provides twelve impulse responses ( $3 \times 4$ ) calculated using different signals. The third plot of Fig. 9 shows one of these orthogonalized

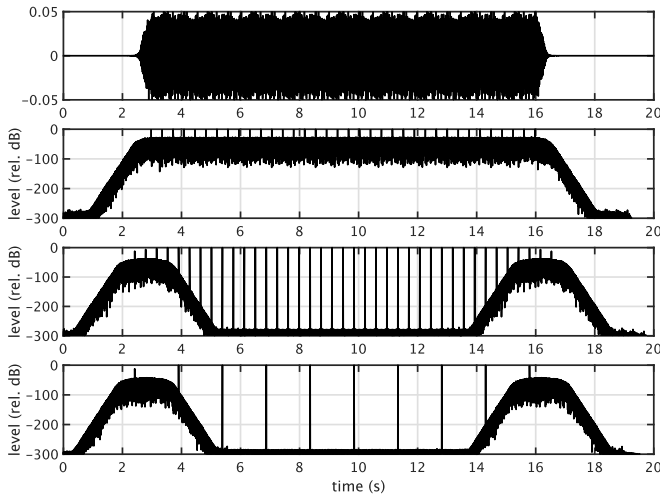


FIG. 9. Mixed signal, recovered signal, orthogonalized signal, and extended signal.

signals. Note that the cross-correlation level is around -300 dB.

Finally, adding three orthogonalized sequences with  $1/4$ ,  $1/4$ , and  $1/2$  weights provides a segment of length  $4N_p$  consisting of a unit impulse. The bottom plot of Fig. 9 shows this extended signal. Therefore, the CAPRICEP-based measuring procedure simultaneously measures thirteen impulse responses for one period. The base test signal in Fig. 9 has six periods with enough suppression of crosscorrelation. Therefore, this base test signal provides 72 ( $12 \times 6$ ) impulse responses and six extended impulse responses.

We take advantage of the base signal periodicity (the period is  $4N_p$ ) and derive an efficient algorithm based on discrete Fourier transform (Kawahara *et al.*, 2022). The proposed tool implements this algorithm using the built-in fast Fourier transform (FFT). The FFT buffer size does not need to be an integer power of two for modern computers because of advancements in algorithms and special-purpose instruction sets, and vector processing mechanisms.

## APPENDIX B: TESTED PITCH EXTRACTORS

We found pitch extractors based on the same algorithm showed different performance depending on their detailed implementation. We listed tested pitch extractors with information regarding their implementation, version, and source locations.

### 1. MATLAB function (LHS, CEP, SRH, LCF, PEF, CREPE)

Scientific computing environment MATLAB has builtin functions for pitch extraction. They consist of classical methods (CEP: cepstrum-based method (Noll, 1967), LCF: LPC-based method (Atal, 1972), and LHS: harmonic summation-based method (Hermes, 1988)),

and recent methods (PEF: (Gonzalez and Brookes, 2014) and SRH: summation of residual harmonics (Drugman and Alwan, 2011)). In addition to these, Deep Learning Toolbox has a deep learning-based method CREPE (Kim *et al.*, 2018).

### 2. YIN (ECKF)

YIN (de Cheveigné and Kawahara, 2002) is an absolute difference-based method originally implemented using MATLAB and C. The original implementation is not compatible with recent MATLAB versions. Therefore, we used a variant implementation in the extended complex Kalman filter-based pitch tracker ECKF (Das *et al.*, 2020).

### 3. SWIPEP

SWIPEP (Camacho and Harris, 2008) uses a harmonic model-based approach originally implemented in MATLAB. It estimates the fundamental frequency of the best matching sawtooth signal. We used the extended version SWIPE' listed in the thesis (Camacho, 2007).

### 4. RAPT (VOICEBOX)

RAPT (Talkin, 1995) for robust processing uses a multi-stage autocorrelation-based method followed by post processing. We used implementation in VOICEBOX: Speech Processing Toolbox for MATLAB (Brooks).

### 5. SRH (COVAREP)

SRH (Hermes, 1988) is a harmonic summation-based method. COVAREP is a repository of speech processing tools (Degottex *et al.*, 2014). We used MATLAB implementation of SRH in COVAREP repository (Degottex *et al.*).

### 6. REAPER

REAPER simultaneously estimate GCI (Glottal Closure Instant), V/UV (voiced or unvoiced), and pitch. We used the open-source implementation (Talkin).

### 7. Praat

Praat is a popular tool for doing phonetics using computers (Boersma and Weenink, 1992–2022). We used recommended procedure “Sound: To Pitch...” which uses the autocorrelation-based method (Boersma, 1993) with the default setting. We used the latest version v.6.2.10 (Boersma and Weenink, 1992–2022).

### 8. openSMILE (SHS, ACF)

openSMILE is widely applied in automatic emotion recognition for affective computing (Eyben *et al.*, 2010a). It has two configuration files for pitch analysis,



prosodyShs.conf which uses the sub-harmonic-sampling method SHS, and prosodyAcf.conf which uses an autocorrelation and cepstrum-based method ACF. We used openSMILE version 3.0.1 for macOS (Eyben *et al.*, 2010b).

## 9. STRAIGHT (NDF, XSX)

STRAIGHT consists of two VOCODER packages, legacy-STRAIGHT (Kawahara *et al.*, 1999) and TANDEM-STRAIGHT (Kawahara *et al.*, 2008b). They use  $f_0$  adaptive spectral envelope recovery. Their  $f_0$  adaptive procedure led to development and refinement of dedicated pitch extractors, NDF (Kawahara *et al.*, 2005) for legacy-STRAIGHT, and XSX (Kawahara *et al.*, 2008a) for TANDEM-STRAIGHT. They are implemented using MATLAB. The legacy-STRAIGHT and NDF is open-source (Kawahara, 2017b) since 2017.

## 10. Harvest (WORLD)

A high-quality VOCODER WORLD (Morise *et al.*, 2016) also use  $f_0$  adaptive spectral envelope recovery. The latest pitch extractor for WORLD is Harvest (Morise, 2017). We used MATLAB implementation version 0.2.4.

## 11. NINJAL, NINJALX2 and YANG

This pitch extractor NINJAL (Kawahara, 2017a; Kawahara *et al.*, 2017) is a refined version of its predecessor YANG (Kawahara, 2016). They use a log-linear filterbank and their instantaneous frequency and residual levels of outputs. We set the smoothing length parameter to 10 ms (named NINJALX2) and 40 ms (named NINJAL: default). The setting of NINJALX2 is the result of fine-tuning enabled by the proposed objective measurement. They are implemented in MATLAB. They are open-source and accessible on YANG (Agiomyrgiannakis *et al.*, 2017) and NINJAL (Kawahara, 2017c).

## APPENDIX C: INTERFACE TO PITCH EXTRACTORS

Figure 10 shows an interface function of a MATLAB function to the measuring program. The pitch extractor is a MATLAB builtin function `pitch` with option setting `CEP` to use the cepstrum-based algorithm (Noll, 1967). Editing relevant lines in this function provides the interface for any pitch extractors implemented using MATLAB.

Figure 11 shows an excerpt of the interface function for calling an external pitch extractor. The pitch extractor is a prosody feature extractor in openSMILE configured using `prosodyShs.conf` which uses the subharmonic sampling algorithm (Hermes, 1988). This excerpt uses the shell escape syntax of MATLAB on macOS. Editing these lines provide means to evaluate any external pitch extractors.

```
function output = pitchCEP(xa, fs)
% Interface function for pitch extractor of Noll's CEPSTRUM
% output = pitchCEP(xa, fs)
% Use the function name "@pitchCEP" for the argument
% of the evaluator
%
% Augment
% xa : test signal with CAPRICEP FM and simulates
% the spectrum of Japanese vowel /a/
% fs : sampling frequency (Hz)
% Output
% output : structure variable with the following fields
% fo : extracted fundamental frequency (Hz)
% tt : discrete temporal locations of fo measurement (s)
% titleStr : string for the first item of the figure title
% filePrefix : string for the beginning of the output files

% LICENSE: refer to LICENSE in this folder

output = struct;
[fo, loc] = pitch(xa, fs, "Method", "CEP", "Range", [70 450]);
output.fo = fo;
output.tt = loc/fs-0.028;
output.titleStr = "CEP ";
output.filePrefix = "pCEP";
end
```

FIG. 10. Interface function for a cepstrum-based pitch extractor implemented as a MATLAB builtin function. The constant -0.028 is for time alignment (Unit: second).

```
audiowrite("testSignal.wav", xa/max(abs(xa))*0.8, fs, ...
"BitsPerSample", 24);
!PATH=$PATH:~/Downloads/opensmile-3.0.1-macos-x64/bin/
!SMILEExtract -C prosodyShs.conf -I testSignal.wav -O testSignal.htk
```

FIG. 11. Interface function for an external function in openSMILE. We added a function to read the output file which uses HTK (Cambridge, 1989–2016) format.

<sup>1</sup>For psychophysical research test signals with the initial phase setting is useful (Patterson, 1987). It may also useful in speech coding (Kleijn, 2003).

<sup>2</sup>In this test, automatic downsampling of NINJAL kicked in. The analysis rate was 44100/6 Hz.

<sup>3</sup>See Supplementary material at [URL will be inserted by AIP] for [the gathered sixteen movies].

Agiomyrgiannakis, Y., Kawahara, H., and Zen, H. (2017). "YANG VOCODER: Yet-ANother-Generalized VOCODER" [muhttps://github.com/google/yang\\_vocoder](https://github.com/google/yang_vocoder), (Last viewed March 17, 2022).

Atal, B. S. (1972). "Automatic speaker recognition based on pitch contours," J. Acoust. Soc. Am. **52**(6B), 1687–1697.

Behroozmand, R., Johari, K., Bridwell, K., Hayden, C., Fahey, D., and Den Ouden, D.-B. (2020). "Modulation of vocal pitch control through high-definition transcranial direct current stimulation of the left ventral motor cortex," Exp. Brain Res. **238**, 1525–1535.

Behroozmand, R., Korzyukov, O., and Larson, C. R. (2012). "ERP correlates of pitch error detection in complex tone and voice auditory feedback with missing fundamental," Brain Res. **1448**, 89–100, doi: [muhttps://doi.org/10.1016/j.brainres.2012.02.012](https://doi.org/10.1016/j.brainres.2012.02.012).

Boersma, P. (1993). "Accurate short-term analysis of the fundamental frequency and the harmonics-to-noise ratio of a sampled sound," in Proc. ICPhS, Vol. 17, pp. 97–110.

Boersma, P., and Weenink, D. (1992–2022). "Praat: doing phonetics by computer [computer program] version 6.2.10" [muhttp://www.praat.org/](http://www.praat.org/), (Last viewed March 17, 2022).

- Brooks, M. "VOICEBOX: Speech processing toolbox for MATLAB" <http://www.ee.ic.ac.uk/hp/staff/dmb/voicebox/voicebox.html>, (Last viewed March 30, 2022).
- Burnett, T. A., Senner, J. E., and Larson, C. R. (1997). "Voice F0 responses to pitch-shifted auditory feedback: a preliminary study," *J. Voice* **11**(2), 202–211.
- Burrascano, P., Laureti, S., Ricci, M., Terenzi, A., Cecchi, S., Spinante, S., and Piazza, F. (2019). "A swept-sine pulse compression procedure for an effective measurement of intermodulation distortion," *IEEE Trans. Instrum. Meas.* **69**(4), 1708–1719.
- Camacho, A. (2007). *SWIPE: A sawtooth waveform inspired pitch estimator for speech and music* (University of Florida Gainesville).
- Camacho, A., and Harris, J. G. (2008). "A sawtooth waveform inspired pitch estimator for speech and music," *J. Acoust. Soc. Am.* **124**(3), 1638–1652, doi: [mu10.1121/1.2951592](https://doi.org/10.1121/1.2951592).
- Cambridge (1989–2016). "The Hidden Markov Toolkit (HTK)" <https://htk.eng.cam.ac.uk/>, (Last viewed March 31, 2022).
- Chang, E. F., Niziolet, C. A., Knight, R. T., Nagarajan, S. S., and Houde, J. F. (2013). "Human cortical sensorimotor network underlying feedback control of vocal pitch," *Proc. Natl. Acad. Sci. U.S.A.* **110**(7), 2653–2658.
- Das, O., Smith III, J. O., and Chafe, C. (2020). "Improved real-time monophonic pitch tracking with the extended complex Kalman filter," *J. Audio Engineering Society* **68**(1/2), 78–86.
- de Cheveigné, A., and Kawahara, H. (2002). "YIN, a fundamental frequency estimator for speech and music," *J. Acoust. Soc. Am.* **111**(4), 1917–1930.
- Degottex, G., Kane, J., Drugman, T., Raitio, T., and Scherer, S. "Covarep: A cooperative voice analysis repository for speech technologies version (after 1.4.1)" <https://github.com/covarep/covarep>, (Last viewed March 30, 2022).
- Degottex, G., Kane, J., Drugman, T., Raitio, T., and Scherer, S. (2014). "COVAREP – A collaborative voice analysis repository for speech technologies," in *Proc. ICASSP*, pp. 960–964, doi: [mu10.1109/ICASSP.2014.6853739](https://doi.org/10.1109/ICASSP.2014.6853739).
- Drugman, T., and Alwan, A. (2011). "Joint robust voicing detection and pitch estimation based on residual harmonics," in *Proc. Interspeech*, pp. 1973–1976, doi: [mu10.21437/Interspeech.2011-519](https://doi.org/10.21437/Interspeech.2011-519).
- Eyben, F., Wöllmer, M., and Schuller, B. (2010a). "openSMILE – the munich versatile and fast open-source audio feature extractor," in *Proc. 18th ACM Multimedia*, pp. 1459–1462.
- Eyben, F., Wöllmer, M., and Schuller, B. (2010b). "openSMILE 3.0: Open-source audio feature extraction" <https://github.com/audeering/opensmile>, (Last viewed March 17, 2022).
- Eyben, F., Wöllmer, M., and Schuller, B. (2010c). "Opensmile: the munich versatile and fast open-source audio feature extractor," in *Proceedings of the 18th ACM international conference on Multimedia*, pp. 1459–1462.
- Farina, A. (2000). "Simultaneous measurement of impulse response and distortion with a swept-sine technique," in *Audio Eng. Soc. Conv. 108*, AES.
- Gonzalez, S., and Brookes, M. (2014). "Pefac - a pitch estimation algorithm robust to high levels of noise," *IEEE/ACM Trans. ASLP* **22**(2), 518–530, doi: [mu10.1109/TASLP.2013.2295918](https://doi.org/10.1109/TASLP.2013.2295918).
- Hain, T. C., Burnett, T. A., Kiran, S., Larson, C. R., Singh, S., and Kenney, M. K. (2000). "Instructing subjects to make a voluntary response reveals the presence of two components to the audio-vocal reflex," *Exp. Brain Res.* **130**(2), 133–141.
- Hermes, D. J. (1988). "Measurement of pitch by subharmonic summation," *J. Acoust. Soc. Am.* **83**(1), 257–264.
- Kadiri, S. R., Alku, P., and Yegnanarayana, B. (2021). "Extraction and utilization of excitation information of speech: A review," *Proceedings of the IEEE*.
- Kawahara, H. (1994). "Interactions between speech production and perception under auditory feedback perturbations on fundamental frequencies," *J. Acoust. Soc. Jpn. (E)* **15**(3), 201–202.
- Kawahara, H. (2016). "Aliasing-free L-F model and its application to an interactive MATLAB tool and test signal generation for speech analysis procedures," in *9th ISCA Speech Synthesis Workshop*, pp. 123–123.
- Kawahara, H. (2017a). "Application of time-frequency representations of aperiodicity and instantaneous frequency for detailed analysis of filled pauses," *Journal of the Phonetic Society of Japan* **21**(3), 63–73, doi: [mu10.24467/onseikenkyu.21.3\\_63](https://doi.org/10.24467/onseikenkyu.21.3_63).
- Kawahara, H. (2017b). "legacy-STRAIGHT" <https://github.com/HidekiKawahara/legacy-STRAIGHT>, (Last viewed March 17, 2022).
- Kawahara, H. (2017c). "YANGstraight source" [https://github.com/HidekiKawahara/YANGstraight\\_source](https://github.com/HidekiKawahara/YANGstraight_source), (Last viewed March 17, 2022).
- Kawahara, H., de Cheveigné, A., Banno, H., Takahashi, T., and Irino, T. (2005). "Nearly defect-free F0 trajectory extraction for expressive speech modifications based on STRAIGHT," in *Proc. Interspeech*, pp. 537–540, doi: [mu10.21437/Interspeech.2005-335](https://doi.org/10.21437/Interspeech.2005-335).
- Kawahara, H., Kato, H., and Williams, J. C. (1996). "Effects of auditory feedback on F0 trajectory generation," in *Proc. ICSLP*, Vol. 1, pp. 287–290, doi: [mu10.1109/ICSLP.1996.607105](https://doi.org/10.1109/ICSLP.1996.607105).
- Kawahara, H., Masuda-Katsuse, I., and de Cheveigné, A. (1999). "Restructuring speech representations using a pitch-adaptive time-frequency smoothing and an instantaneous-frequency-based F0 extraction," *Speech Communication* **27**(3-4), 187–207.
- Kawahara, H., Matsui, T., Yatabe, K., Sakakibara, K.-I., Tsuzaki, M., Morise, M., and Irino, T. (2021a). "Implementation of interactive tools for investigating fundamental frequency response of voiced sounds to auditory stimulation," in *Proc. APSIPA ASC*, pp. 897–903.
- Kawahara, H., Matsui, T., Yatabe, K., Sakakibara, K.-I., Tsuzaki, M., Morise, M., and Irino, T. (2021b). "Mixture of orthogonal sequences made from extended time-stretched pulses enables measurement of involuntary voice fundamental frequency response to pitch perturbation," in *Proc. Interspeech 2021*, pp. 3206–3210.
- Kawahara, H., Morise, M., Takahashi, T., Nisimura, R., Banno, H., and Irino, T. (2008a). "A unified approach for F0 extraction and aperiodicity estimation based on a temporally stable power spectral representation," in *Proc. ISCA ITRW on Speech Analysis and Processing for Knowledge Discovery*, p. paper 043.
- Kawahara, H., Morise, M., Takahashi, T., Nisimura, R., Irino, T., and Banno, H. (2008b). "Tandem-straight: A temporally stable power spectral representation for periodic signals and applications to interference-free spectrum, f0, and aperiodicity estimation," in *Proc. ICASSP*, pp. 3933–3936, doi: [mu10.1109/ICASSP.2008.4518514](https://doi.org/10.1109/ICASSP.2008.4518514).
- Kawahara, H., Sakakibara, K.-I., Morise, M., Banno, H., and Toda, T. (2017). "Accurate estimation of fo and aperiodicity based on periodicity detector residuals and deviations of phase derivatives," in *Proc. APSIPA ASC*, pp. 12–15.
- Kawahara, H., and Yatabe, K. (2021). "Cascaded all-pass filters with randomized center frequencies and phase polarity for acoustic and speech measurement and data augmentation," *Proc. ICASSP2021* 306–310.
- Kawahara, H., Yatabe, K., Sakakibara, K.-I., Kitamura, T., Banno, H., and Morise, M. (2022). "An objective test tool for pitch extractors' response attributes," in *Proc. Interspeech*, (submitted).
- Kim, J. W., Salamon, J., Li, P., and Bello, J. P. (2018). "CREPE: A convolutional representation for pitch estimation," in *Proc. ICASSP*, pp. 161–165.
- Kleijn, W. B. (2003). "Signal processing representations of speech," *IEICE TRANSACTIONS on Information and Systems* **86**(3), 359–376.
- Larson, C. R., and Robin, D. A. (2016). "Sensory processing: Advances in understanding structure and function of pitch-shifted auditory feedback in voice control," *AIMS Neurosci.* **3**(1), 22–39, doi: [mu10.3934/Neuroscience.2016.1.22](https://doi.org/10.3934/Neuroscience.2016.1.22).
- Maekawa, K. (2003). "Corpus of spontaneous Japanese: its design and evaluation," in *Proc. ISCA/IEEE Workshop on Spontaneous Speech Processing and Recognition*, p. paper MMO2.
- McAulay, R., and Quatieri, T. (1986). "Speech analysis/synthesis based on a sinusoidal representation," *IEEE Transactions on Acoustics, Speech, and Signal Processing* **34**(4), 744–754.
- Morise, M. (2017). "Harvest: A high-performance fundamental frequency estimator from speech signals," in *Proc. Interspeech*, pp. 2321–2325, doi: [mu10.21437/Interspeech.2017-68](https://doi.org/10.21437/Interspeech.2017-68).
- Morise, M., Yokomori, F., and Ozawa, K. (2016). "WORLD: A vocoder-based high-quality speech synthesis system for real-time

- applications,” IEICE Trans. Information and Systems **99**(7), 1877–1884.
- Noll, A. M. (1967). “Cepstrum pitch determination,” J. Acoust. Soc. Am. **41**(2), 293–309, doi: [mu10.1121/1.1910339](https://doi.org/10.1121/1.1910339).
- Patel, S., Lodhavia, A., Frankford, S., Korzyukov, O., and Larson, C. R. (2016). “Vocal and neural responses to unexpected changes in voice pitch auditory feedback during register transitions,” J. Voice **30**(6), 772.e33–772.e40, doi: [muhttps://doi.org/10.1016/j.jvoice.2015.11.012](https://doi.org/10.1016/j.jvoice.2015.11.012).
- Patterson, R. D. (1987). “A pulse ribbon model of monaural phase perception,” The Journal of the Acoustical Society of America **82**(5), 1560–1586.
- Peng, D., Lin, Q., Chang, Y., Jones, J. A., Jia, G., Chen, X., Liu, P., and Liu, H. (2021). “A causal role of the cerebellum in auditory feedback control of vocal production,” Cerebellum 1–12.
- Schroeder, M. (1970). “Synthesis of low-peak-factor signals and binary sequences with low autocorrelation,” IEEE Trans. Inf. Theory **16**(1), 85–89.
- Schuller, B., and Batliner, A. (2013). *Computational paralinguistics: emotion, affect and personality in speech and language processing* (John Wiley & Sons).
- Sivasankar, M., Bauer, J. J., Babu, T., and Larson, C. R. (2005). “Voice responses to changes in pitch of voice or tone auditory feedback,” J. Acoust. Soc. Am. **117**(2), 850–857, doi: [mu10.1121/1.1849933](https://doi.org/10.1121/1.1849933).
- Stan, G.-B., Embrechts, J.-J., and Archambeau, D. (2002). “Comparison of different impulse response measurement techniques,” J. Audio Eng. Soc. **50**(4), 249–262.
- Talkin, D. “REAPER: Robust epoch and pitch estimator” [muhttps://github.com/google/REAPER](https://github.com/google/REAPER), (Last viewed March 21, 2022).
- Talkin, D. (1995). “A robust algorithm for pitch tracking (RAPT),” in *Speech coding and synthesis*, edited by D. Talkin and W. B. Kleijn (Elsevier Science), pp. 497–512.
- The Mathworks, I. (2022). *MATLAB version 9.12.0.1884302 (R2022a)*, The Mathworks, Inc., Natick, Massachusetts.
- Titze, I. R. (1993). “Comparison of Fo extraction methods for high-precision voice perturbation measurements an optimizer-simulator for phonosurgery view project,” Article in Journal of Speech and Hearing Research **36**, 1120–1133, [muhttps://www.researchgate.net/publication/15083731](https://www.researchgate.net/publication/15083731), doi: [mu10.1044/jshr.3606.1120](https://doi.org/10.1044/jshr.3606.1120).
- Tourville, J. A., Reilly, K. J., and Guenther, F. H. (2008). “Neural mechanisms underlying auditory feedback control of speech,” NeuroImage **39**(3), 1429 – 1443, doi: [muhttps://doi.org/10.1016/j.neuroimage.2007.09.054](https://doi.org/10.1016/j.neuroimage.2007.09.054).
- Välimäki, V., Lehtonen, H. M., and Takanen, M. (2013). “A perceptual study on velvet noise and its variants at different pulse densities,” IEEE Trans. Audio, Speech, Lang. Process. **21**(7), 1481–1488, doi: [mu10.1109/TASL.2013.2255281](https://doi.org/10.1109/TASL.2013.2255281).
- Zarate, J. M., Wood, S., and Zatorre, R. J. (2010). “Neural networks involved in voluntary and involuntary vocal pitch regulation in experienced singers,” Neuropsychologia **48**(2), 607–618.